Removal of Heavy Metal Chromium in Groundwater by Sulfidated and Carboxymethyl Cellulose Modified Nanoscale Zero-valent Iron

Linminhuizhi MA [1], Jiwei JIA [2]*, Qiying FAN [3], Beiyi XU [3]

[1] *Water Resources Department, Taizhou Hydrology and Water Resources Survey Bureau of Jiangsu Province, Taizhou, Jiangsu, 225300, China*
[2] *Nanjing Yuangu Water Industry Company Limited, Nanjing, Jiangsu, 210044, China*
[3] *College of Transportation Science & Engineering, Nanjing Tech University, Nanjing, Jiangsu, 211816, China*

http://doi.org/10.5755/j02.ms.39630

Received 29 November 2024; accepted 29 January 2025

In this study, nanoscale zero-valent iron (nZVI) was investigated for its effectiveness in removing chromium, a major groundwater contaminant. To enhance nZVI's removal performance, sulfurization and sodium carboxymethyl cellulose (CMC) modifications were applied. Three preparation methods were used to create modified nZVI materials with distinct structures, and their removal efficiencies were compared. Results showed that the nZVI modified via surface corrosion achieved the highest removal efficiency. Furthermore, the study explored the effects of various factors on the removal efficiency, including the molar ratio of sulfurizing agent to iron, initial pH, reaction temperature, the dosage of modified nZVI, and the initial concentration of hexavalent chromium. The results showed that the highest chromium removal rate (96.97 %) was achieved when the molar ratio of sulfurizing agent to iron was 0.4, the initial pH was 3, the reaction temperature was 25 ℃, the dosage of modified nZVI was 52 mg/L, and the initial hexavalent chromium concentration was 12 mg/L. After three cycles of reuse, the modified nZVI material still maintained a removal rate of 94.73 %. Additionally, the presence of various ions in wastewater was found to influence the removal efficiency. The effect of anions was minimal and could be neglected, while the presence of cations, particularly Mg^{2+}, had a significant impact on removal performance. Under conditions simulating multi-ion groundwater, the modified nZVI material demonstrated a removal rate of up to 90.25 % for hexavalent chromium, highlighting its potential for practical applications.
Keywords: nZVI, nanometer, groundwater, pollutants, remove, chromium.

1. INTRODUCTION

Freshwater is the main source of water for human daily life and economic activities [1]. Groundwater is an important freshwater resource, which has advantages such as good water quality, stable water volume, and relatively low extraction costs [2]. However, with the development of society and the uncontrolled use of fertilizers and pesticides by humans, pollutants in groundwater are gradually increasing, leading to a decrease in groundwater quality. Groundwater pollution is mainly a composite pollution, among which the most critical pollutants include heavy metals, organic pollution, and "three nitrogen" [3]. Protecting groundwater resources is not only related to human water safety, but also to the stability and biodiversity of ecosystems. Therefore, removing pollutants from groundwater becomes particularly important. Chromium is one of the main sources of heavy metal pollution in groundwater. Hexavalent chromium is widely recognized as a human carcinogen [4]. Commonly used methods for hexavalent chromium pollution in groundwater have extraction treatment technology, permeable reaction barrier technology, in-situ reaction zone remediation technology, and nano Zero Valent Iron (nZVI) [5, 6].

Yang et al. designed a bimetallic iron manganese oxide for groundwater remediation and used it as a catalyst for oxygen ketone groups in groundwater remediation. The results showed that sulfate radicals and hydroxyl radicals exerted crucial functions in the degradation of trichloroethylene [7]. Brumovský et al. designed a new method for synthesizing sulfurized nZVI to address the groundwater pollutants. This method is applicable to nZVI particles treated with sodium sulfide in a concentrated slurry. The removal of trichloroethylene increased by 12 times, the electronic efficiency increased by 7 times, and the chlorine equilibrium was close to 100 % [8]. Huang et al. adopted an in-situ anaerobic treatment method to remediate petroleum hydrocarbon pollution in groundwater, using microbial agents with quinone respiration ability to remove petroleum hydrocarbons. In the multi well survey, the removal rates of petroleum hydrocarbons after 63 days were 95 %, 89 %, and 94 %, respectively, and the removal rate of downstream monitoring wells of groundwater was relatively high, reaching up to 76.5 % [9 – 11]. Ishag et al. designed a new nZVI/molybdenum disulfide composite material for the uranium in polluted wastewater. The composite material had a high specific surface area and uniform nZVI distribution, with maximum adsorption of 71.8 mg/gat [12 – 15].

However, current research and methods also have certain shortcomings, such as the high operating cost of extraction and treatment technology, and the rebound in pollutant concentration. The permeable reactive barrier technology has limitations in the treatment of deep polluted

* Corresponding author: J. Jia
E-mail: *jiajiwei@nywicl.cn*

groundwater. The migration ability of nZVI is limited by particle aggregation, which is prone to interact with certain chemical components in groundwater, reducing reaction efficiency. In order to remove hexavalent chromium heavy metal pollutants from groundwater, nZVI material is selected and sulfurization technology and carboxy methyl cellulose (CMC) are introduced to modify nZVI nanomaterials. The research aims to improve the performance of nZVI materials and their removal efficiency for hexavalent chromium, reduce heavy metal pollution in groundwater, and promote the development of groundwater treatment and protection work. The innovation of the research is reflected in the combination of vulcanization technology and CMC. Three methods are used to prepare modified nZVI nanomaterials, improving the removal efficiency of modified nZVI nanomaterials.

2. METHODS AND MATERIALS

2.1. Reagents

The primary reagents used in this study include ferrous sulfate heptahydrate, sodium borohydride, sodium sulfide, anhydrous ethanol, sodium dichromate dihydrate, diphenylamine, sodium hydroxide, concentrated sulfuric acid, CMC, $CaCl_2$, $FeCl_3$, $MgCl_2 \cdot 6H_2O$, $MnCl_2$, NaCl, Na_2SO_4, $NaHCO_3$, and $NaNO_3$. Sodium dichromate dihydrate was sourced from Merck KGaA (Darmstadt, Germany), while the remaining reagents were obtained from Shanghai Aladdin Biochemical Technology Co., Ltd. All reagents were of analytical grade.

2.2. Preparation of nZVI

The preparation reaction device diagram of nZVI is shown in Fig. 1. To synthesize nZVI, 30 mL of a sodium borohydride solution (3.6 mmol) was added dropwise to 90 mL of an ethanol solution (30 % v/v) containing ferrous sulfate (2.4 mmol) under a nitrogen atmosphere, with vigorous stirring throughout the process. After the addition was complete, the reaction mixture was stirred for an additional 45 min to allow for the release of hydrogen gas produced during the reaction. The resulting precipitate was washed three times, first with deoxygenated water and then with deoxygenated ethanol. Finally, the material was dried in a vacuum freeze dryer for 36 h. The nZVI product was sealed and stored for future use.

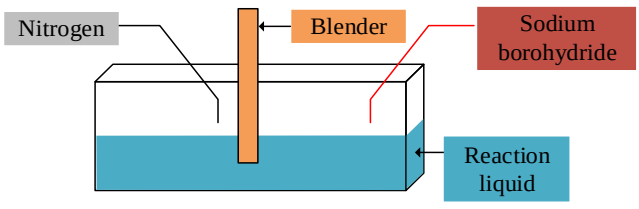

Fig. 1. Preparation reaction device diagram of nZVI

2.3. Preparation of sulfidated nZVI

Under a nitrogen atmosphere, a specific amount of sodium sulfide was added to an nZVI suspension to create mixed solutions with varying S/Fe ratios, maintaining a total iron concentration of 1.5 g/L. Dilute sulfuric acid (0.2 mol/L) was then added dropwise to adjust the pH of the system to approximately 7.6. The mixture was sealed and placed in a constant temperature shaker at 25 °C, and shaken at 250 rpm for 5 hours. The resulting product was separated with a magnet, washed three times each with deoxygenated water and deoxygenated ethanol, and vacuum freeze-dried. The final product was stored in a sealed container for future use.

2.4. Preparation of CMC-nZVI

A solution of 83 mL containing 2.7 mmol of ferrous sulfate was added to 38 mL of CMC solution (1.5 % w/w) and stirred for 40 minutes to form the Fe(II)-CMC complex. Then, 30 mL of sodium borohydride solution containing 5.4 mmol was slowly added dropwise to the Fe(II)-CMC mixture. Throughout the reaction, vigorous stirring was maintained using a magnetic stirrer, and nitrogen gas was continuously purged into the system to prevent oxidation. After the complete addition of reagents, nitrogen purging continued for an additional 45 minutes to release the hydrogen gas produced during the reaction. The resulting CMC-nZVI suspension was sealed in a serum bottle and used on the same day it was prepared.

2.5. Preparation of modified nZVI nanomaterials

A 30 mL mixed solution containing sodium borohydride (3.5 mmol) and sodium sulfide (0.9 mmol) was added dropwise to a mixture of 120 mL of ferrous sulfate (2.7 mmol) and CMC solution. The reaction was carried out under nitrogen protection with continuous vigorous stirring to ensure thorough mixing and reaction.

Sodium borohydride (3.5 mmol) was added dropwise to the Fe(II)-CMC mixture. After the reaction was completed, Sodium sulfide solution (0.9 mmol) was gradually added.

A specific amount of Sodium sulfide was added to 150 mL of freshly prepared CMC-nZVI suspension (with a total iron concentration of 1.5 g/L) to achieve various S/Fe ratios. The pH of the system was adjusted to approximately 7.6. The suspension was purged with nitrogen gas and placed on a thermostatic shaker at 25 ℃ for 36 hours. After the reaction, the suspension was sealed and stored for later use.

2.6. Material characterization

The morphology and structure of various materials were observed using a SU8010 scanning electron microscope (SEM; HITACHI, Japan). Infrared spectra of the samples were obtained using a Thermo Nicolet iS10 spectrometer (Thermo Nicolet Corp., Madison, WI, USA). X-ray diffraction (XRD) analysis was conducted using a Rigaku D/Max2500 instrument equipped with Cu K_α radiation at 40 kV and 250 mA. Raman spectra were obtained using a Labram-010 spectrometer (France) with a 632 nm excitation laser. Additionally, the transmittance of the samples was measured using a UV – vis spectrophotometer (model UV-2450, Shimadzu, Japan).

2.7. Stability testing

To investigate the stability of the modified nZVI nanomaterials, sedimentation experiments were conducted. Oxygen-free water was added to nanoparticle suspensions to prepare four types of suspensions: nZVI, sulfurized nZVI,

CMC-nZVI, and modified nZVI nanomaterials. The transmittance at a wavelength of 508 nm was measured for each suspension to compare their stability.

2.8. Experimental factors affecting removal efficiency of modified nZVI nanomaterials

To evaluate the impact of several variables on pollutant removal efficiency, experiments were designed to study the effects of sulfurizing agent-to-iron molar ratio, initial pH, reaction temperature, dosage of modified nZVI nanomaterials, and initial concentration of hexavalent chromium (Cr(VI)). Six molar ratios of sulfurizing agent to iron were used: 0, 0.08, 0.16, 0.24, 0.32, and 0.40. The initial pH was adjusted in the range of 2 to 11. Reaction temperatures were set to 0 °C, 18 °C, 25 °C, and 36 °C, while the dosage of modified nZVI nanomaterials was varied at 12 mg/L, 22 mg/L, 32 mg/L, 42 mg/L, and 52 mg/L. The initial Cr(VI) concentration was tested at 12 mg/L, 32 mg/L, 42 mg/L, 52 mg/L, and 102 mg/L. The concentration of Cr(VI) during the reaction was measured using the diphenylcarbazide spectrophotometric method [16]. Moreover, the study examined the influence of common groundwater ions – including Ca^{2+}, Mg^{2+}, Mn^{2+}, Cl^-, $HCO_3^-$and NO_3^- – on the Cr(VI) removal performance of modified nZVI nanomaterials.

2.9. Reaction kinetics

A study on reaction kinetics was also conducted to further understand the material behavior. The dynamic equation is shown in Eq. 1 [17, 18]:

$$\frac{T}{B_T} = \frac{1}{L_2 B_r^2} + \frac{T}{B_r}, \quad (1)$$

where T is the time, min; B_r is the equilibrium adsorption capacity, mg/g; L_2 is the Pseudo Second Order Kinetic Adsorption (PSOKA) rate constant, (g/mg·min); B_T is the adsorption capacity at T, mg/g.

2.10. Regeneration studies

The regeneration process of modified nZVI nanomaterials requires the removal of hexavalent chromium ions from the adsorbent's surface at the end of batch experiments to enable their reuse. Following adsorption experiments, the residual materials on the modified nZVI nanomaterials were first washed with deionized water and then subjected to centrifugation. The resulting precipitate was added to 40 mL of 0.1 M HNO_3 solution and shaken at 145 rpm for 30 minutes at 25 ℃. After centrifugation, the modified nZVI nanomaterials were collected and repeatedly washed with deionized water to neutralize the acidic conditions. Subsequently, the recovered materials were used for the next round of adsorption experiments. This recycling process was conducted three times, with adsorption data recorded for each cycle.

2.11. Experimental study on the remediation of simulated Cr(VI)-contaminated groundwater using modified nZVI nanomaterials

Simulated groundwater was prepared, with its quality parameters listed in Table 1. A Cr(VI) stock solution was added to 50 mL of simulated groundwater and mixed thoroughly. Nitrogen gas was bubbled through the solution for 20 minutes to ensure a low-oxygen environment. Subsequently, 5 mL of modified nZVI nanomaterial suspension was introduced, and the mixture was agitated under a nitrogen headspace. Samples were taken at regular intervals for measurement, and the removal efficiency of hexavalent chromium was calculated.

Table 1. Hydrochemical parameters of polluted groundwater

Parameter	Content, mg/L	Parameter	Content, mg/L	Parameter	Content, mg/L
Sulfate ion	98.0	Dissolved oxygen	8.18	Potassium ion	17.2
Sodium ion	69.6	Divalent calcium ion	70.2	Divalent magnesium ion	25.3
Chloride ion	122.1	Nitrate radical	26.9	Bicarbonate ion	162.4

3. RESULTS

3.1. Comparison of structure and adsorption properties of modified nZVI nanomaterials synthesized by different methods

The SEM images of the modified nZVI nanomaterials prepared by the three methods are shown in Fig. 2.

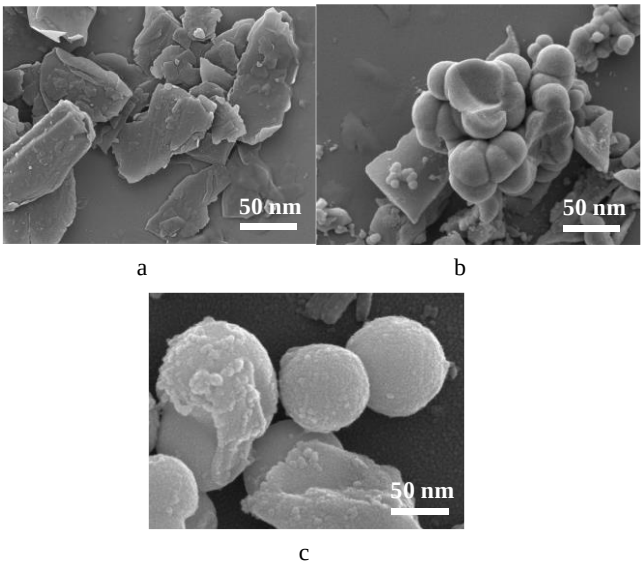

Fig. 2. SEM images of modified nZVI nanomaterials synthesized using three different methods: a – pre-sulfurization method; b – surface deposition method; c – surface corrosion method

As observed in Fig. 2 a, the material prepared via the pre-sulfidation method does not exhibit a spherical core-shell structure, with particle sizes ranging from 50 to 150 nm. The nucleation process of the nZVI material was interrupted. According to Fig. 2 b, the SEM of the modified nZVI nanomaterial prepared by the surface deposition method shows flakier FeS substances, with sizes ranging from 5 to 80 nm. As shown in Fig. 2 c, the modified nZVI nanomaterials prepared by the surface corrosion method have a flaky shell structure on their surface, with sizes ranging from 50 to 100 nm. The figure indicates that the

modified nZVI nanomaterials prepared by the surface corrosion method exhibit better performance and more uniformity.

According to Fig. 3, the removal rates of modified nZVI nanomaterials prepared by the three methods were higher than those of CMC-nZVI materials. For example, the maximum removal rates corresponding to the surface corrosion method, surface deposition method, and pre sulfurization method are 96.97 %, 96.33 %, and 89.01 %, respectively. The maximum removal rate of hexavalent chromium in CMC-nZVI material was 75.21 %, which was 24.76 %, 21.12 %, and 13.80 % lower than the maximum removal rates of materials prepared by the three methods, respectively. The modified nZVI nanomaterials prepared by surface corrosion method have better removal performance. Therefore, the modified nZVI nanomaterials in the subsequent results are all prepared by the surface corrosion method.

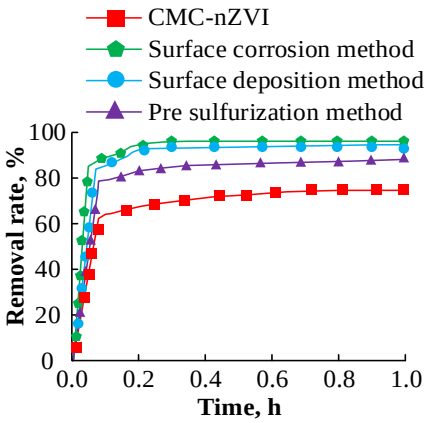

Fig. 3. The influence of different preparation methods on material properties

3.2. Characterization of modified nZVI nanomaterials

The FTIR comparison of different materials is shown in Fig. 4. In Fig. 4, CMC, CMC-nZVI, and modified nZVI nanomaterials were all different. Compared with the characteristic peak of CMC, the wave numbers corresponding to the characteristic peak of modified nZVI nanomaterials increased. For example, on the first characteristic peak, the wave number corresponding to CMC material was 3458 cm^{-1}, while the wave numbers of CMC-nZVI and modified nZVI nanomaterials were both 3439 cm^{-1}. In addition, CMC materials had corresponding characteristic peaks at wave numbers 2994 cm^{-1} and 2854 cm^{-1}, while CMC-nZVI and modified nZVI nanomaterials did not have corresponding characteristic peaks at these two wave numbers. In summary, the fusion of CMC material and nZVI or sulfurized nZVI material is both on the surface layer.

The XRD comparison of different materials is shown in Fig. 5. From Fig. 5, it can be seen that the nZVI, CMC nZVI, and modified nZVI nanomaterials all exhibit diffraction peaks of Fe, indicating the presence of Fe in the material. Meanwhile, the CMC nZVI material exhibited diffraction peaks of Fe_3O_4, indicating a certain degree of oxidation. The modified nZVI nanomaterials exhibit diffraction peaks of Na_2SO_4, with SO_4^{2-} ions mainly provided by Fe_3O_4.

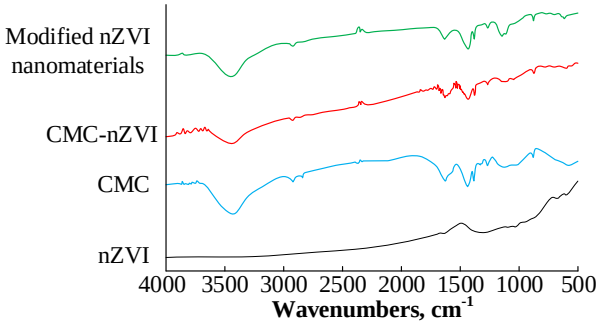

Fig. 4. FTIR spectra of different materials

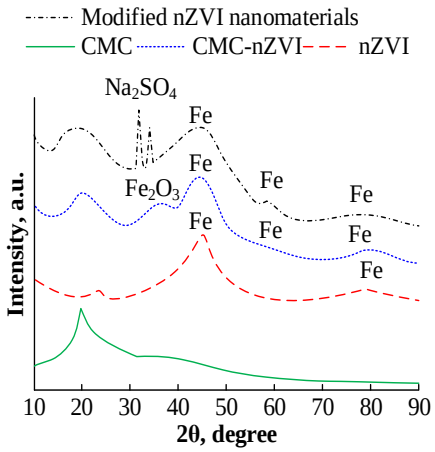

Fig. 5. XRD patterns of different materials

The Raman spectra for different materials are shown in Fig. 6. By analyzing Fig. 6a and Fig. 6 b, it is evident that after modification, the main peaks of the nZVI material shifted either to the left or to the right. Additionally, the five main characteristic peaks of both materials correspond to one another. No characteristic peak of magnetite was detected in the Raman spectra.

3.3. Stability of modified nZVI nanomaterials

The transmittance of nanoparticle suspensions at a wavelength of 508 nm was measured over time using a UV-Vis spectrophotometer. The light transmittance of nanoparticle suspensions of various materials is shown in Fig. 7. From Fig. 7, with the increase of time, the transmittance of nZVI and sulfurized nZVI suspensions both showed a synchronous growth trend, while the transmittance of CMC-nZVI and modified nZVI nanomaterial suspensions first stabilized, then increased, and decreased. In addition, the maximum transmittance values of the four material suspensions were 71.57 %, 59.92 %, 6.89 %, and 2.54 %, respectively. Vulcanization can appropriately alleviate particle aggregation and sedimentation.

3.4. Influencing factors of adsorption properties of modified nZVI nanomaterials

The effect of the sulfurizing agent-to-iron molar ratio on the performance of modified nZVI nanomaterials is illustrated in Fig. 8. Specifically, Fig. 8 a displays the

removal rates of hexavalent chromium over time for both modified nZVI and sulfurized nZVI materials, while Fig. 8 b presents the removal rates of hexavalent chromium as a function of the sulfurizing agent-to-iron molar ratio for the two materials.

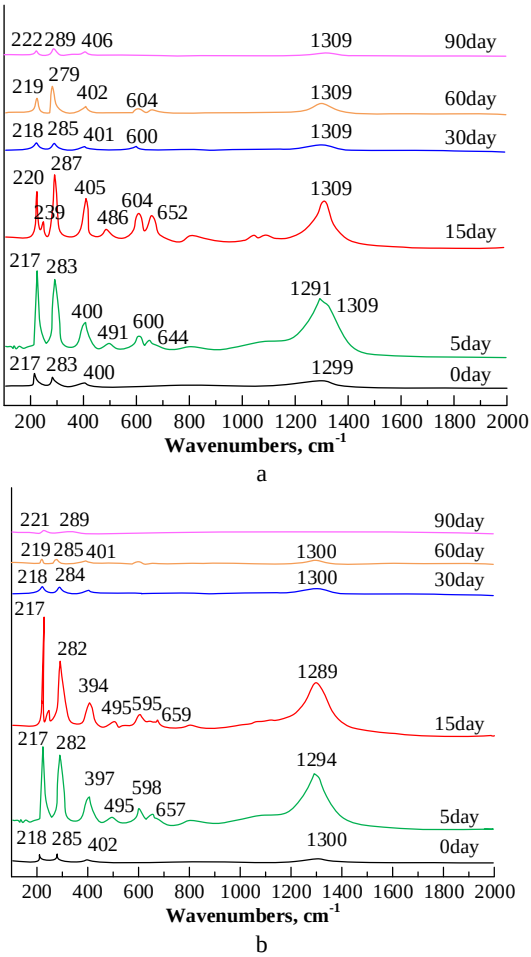

Fig. 6. Raman spectra for different materials: a – nZVI; b – modified nZVI nanomaterials

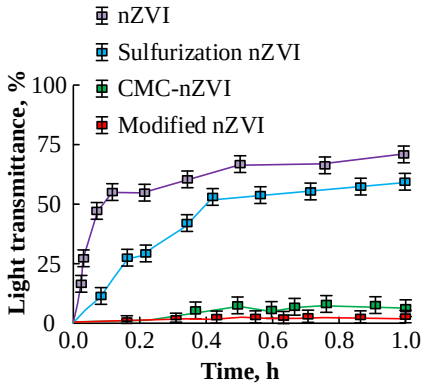

Fig. 7. The light transmittance of nanoparticle suspensions of various materials

In Fig. 8 a, it is evident that at various sulfurizing agent-to-iron molar ratios, the removal rate of hexavalent chromium using modified nZVI nanomaterials initially increases rapidly before reaching a slower growth phase over time. This material quickly achieved a removal rate near its maximum value, significantly outpacing the sulfurized nZVI materials. Additionally, at the same sulfurizing agent-to-iron molar ratios, the maximum removal rate of hexavalent chromium for modified nZVI nanomaterials exceeded that of sulfurized nZVI materials. For instance, at a sulfurizing agent-to-iron molar ratio of 0.4, the removal rates for the two materials were 96.97 % and 58.75 %, respectively.

As shown in Fig. 8 b, the removal rate for both materials initially increases with rising sulfurizing agent-to-iron molar ratios, followed by a decline at higher ratios. The maximum removal rates achieved by the two materials were 96.97 % and 71.85 %, corresponding to sulfurizing agent-to-iron molar ratios of 0.4 and 0.24, respectively. Overall, the results indicate that modified nZVI nanomaterials exhibit superior heavy metal removal performance, particularly at an optimal sulfurizing agent-to-iron molar ratio of 0.4.

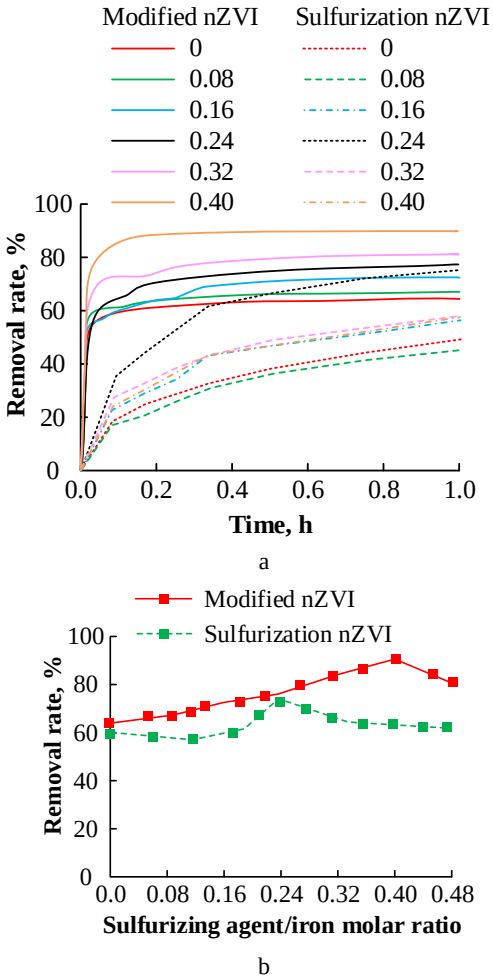

Fig. 8. Effect of sulfurizing agent-to-iron molar ratio on the properties of modified nZVI nanomaterials: a – variation in removal rate over time; b – removal rate as a function of sulfurizing agent-to-iron molar ratio

The effect of initial pH on the removal rate of different materials is displayed in Fig. 9. From Fig. 9 a, with the increase of initial pH, the pH of modified nZVI nanomaterials, CMC-nZVI, and nZVI materials after reaction also increased synchronously. In addition, the maximum solution pH values after the reaction of the three materials were 11.3, 9.46, and 10.58. In Fig. 9 b, the removal rates of hexavalent chromium decreased with the increase of initial pH. The removal rate of hexavalent

chromium for modified nZVI nanomaterials exceeded CMC-nZVI and nZVI materials. The removal rate of modified nZVI nanomaterials was always greater than 50 %, with a maximum value of 96.97 %. The maximum removal rates of CMC-nZVI and nZVI materials were 49.98 % and 42.01 %, respectively, which were significantly lower than the removal rate of modified nZVI nanomaterials. The initial pH values corresponding to the maximum removal rates of the three materials were all 3. In summary, when the initial pH value was 3, the higher removal rate in groundwater by the modified nZVI material. At the same initial pH value, the performance of modified nZVI nanomaterials is better, which can efficiently remove hexavalent chromium.

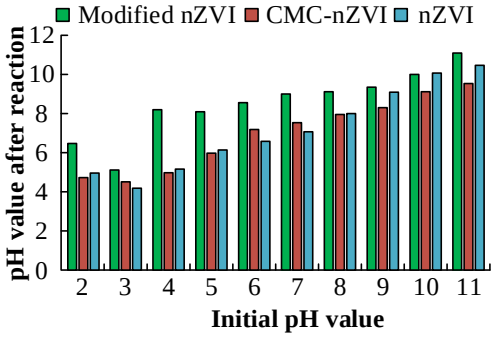

a

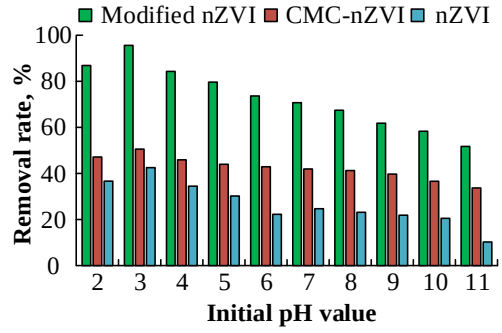

b

Fig. 9. Comparison of the effect of initial pH on the removal efficiency of different materials: a – effect of initial pH on the pH value after the reaction; b – effect of initial pH on the removal efficiency

The effect of different temperatures on the removal efficiency and reaction kinetics of modified nZVI nanomaterials is shown in Fig. 10. As shown in Fig. 10 a, at the same reaction time, as the temperature increases, the maximum removal rate first increases and then decreases. In addition, the removal rates at 0 °C, 18 °C, 25 °C, and 36 °C all tended to stabilize after about 10 minutes of reaction, and the maximum removal rates corresponding to each were 84.58 %, 84.59 %, 96.97 %, and 86.42 %, respectively. Appropriate high temperature can enhance the removal effect of modified nZVI nanomaterials on hexavalent chromium. From Fig. 10 b, as the temperature increases, the PSOKA constant L_2 and the equilibrium adsorption capacity first increase and then decrease. The corresponding L_2 at 0 °C, 18 °C, 25 °C, and 36 °C were 0.514×10^{-2} g/mg·min, 1.309×10^{-2} g/mg·min, 3.751×10^{-2} g/mg·min, and 3.612×10^{-2} g/mg·min. The equilibrium adsorption capacities were 3.570×10^{2} mg/g, 3.570×10^{2} mg/g, 3.923×10^{2} mg/g, and 3.695×10^{2} mg/g, respectively. Overall, the removal effect of modified nZVI nanomaterials at 25 °C is better.

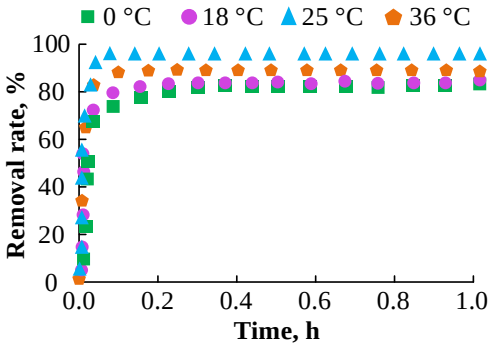

a

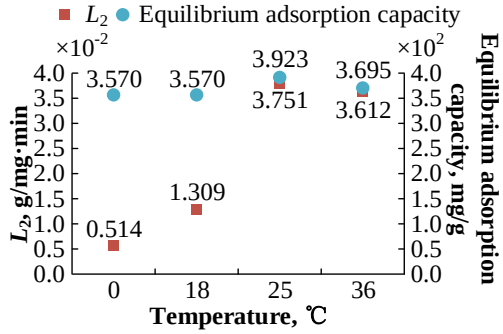

b

Fig. 10. Effect of temperature on the removal efficiency and reaction kinetics of modified nZVI nanomaterials: a – impact on removal efficiency; b – impact on reaction kinetics

The effect of different adsorbent dosages on the removal performance of modified nZVI nanomaterials is shown in Fig. 11. From Fig. 11 a, the concentration of hexavalent chromium rapidly decreased after adding modified nZVI nanomaterials. Meanwhile, the higher the dosage of modified nZVI nanomaterials, the greater the decrease in hexavalent chromium concentration. The minimum concentrations of hexavalent chromium at five different dosages were 11.50 mg/L, 8.01 mg/L, 5.17 mg/L, 3.12 mg/L, and 0.01 mg/L, respectively. In Fig. 11 b, with the increase of the dosage of modified nZVI nanomaterials, the corresponding removal rate of hexavalent chromium also increased synchronously. When the reaction time was 10 minutes, the removal rate of 52 mg/L modified nZVI nanomaterials was 96.77 %, which was 58.56 %, 41.02 %, 28.44 %, and 14.51 % higher than the removal rates at 12 mg/L, 22 mg/L, 32 mg/L, and 42 mg/L. Similarly, at 60 minutes, the removal rate of 96.34 % corresponding to 52 mg/L modified nZVI nanomaterials was also higher than the removal rates in the other four cases.

The effect of different initial hexavalent chromium concentrations on the removal efficiency of modified nZVI nanomaterials are presented in Fig. 12. In Fig. 12 a, after adding modified nZVI nanomaterials, the removal rate showed a rapid increase, and the subsequent changes were not significant.

At the same reaction time, the lower the initial hexavalent chromium concentration, the higher the corresponding removal rate.

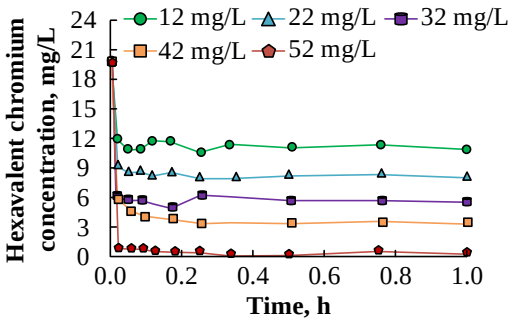

a

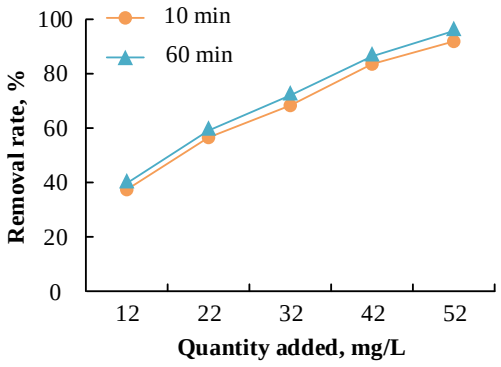

b

Fig. 11. Effect of dosage on the removal performance of modified nZVI nanomaterials: a – impact on hexavalent chromium concentration; b – impact on removal rate

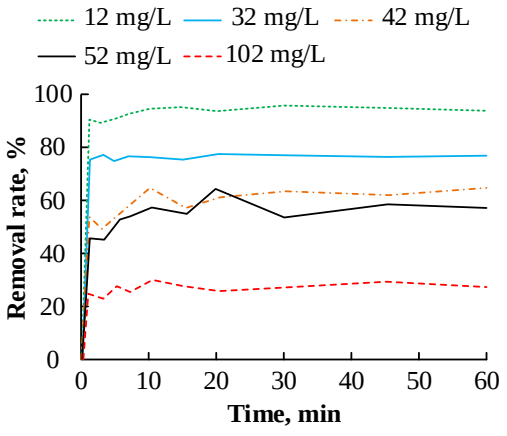

a

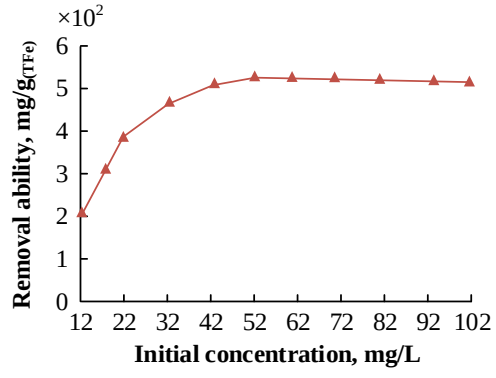

b

Fig. 12. Properties of modified nZVI nanomaterials at varying initial hexavalent chromium concentrations: a – effect on removal rate; b – effect on removal capacity

For example, at 10 minutes, the removal rates of modified nZVI nanomaterials at initial hexavalent chromium concentrations of 12 mg/L, 32 mg/L, 42 mg/L, 52 mg/L, and 102 mg/L were 96.97 %, 76.88 %, 63.73 %, 53.64 %, and 28.45 %, respectively. According to Fig. 12 b, as the hexavalent chromium increased, the removal amount gradually increased first and then began to decrease. The maximum and minimum removal amounts were 530.42 mg/g (TFe) and 200.00 mg/g (TFe), respectively. The corresponding initial hexavalent chromium concentrations were 52 mg/L and 12 mg/L. Overall, the lower the initial concentration, the higher the removal rate of modified nZVI nanomaterials.

To further verify the performance of the modified nZVI nanomaterials designed for research, recyclability experiments were conducted, and the experimental data were organized and analyzed. In the recyclability experiment, the modified nZVI nanomaterials were recycled three times, with each experiment lasting for 60 minutes. The experimental results of the recyclability of modified nZVI nanomaterials are shown in Fig. 13.

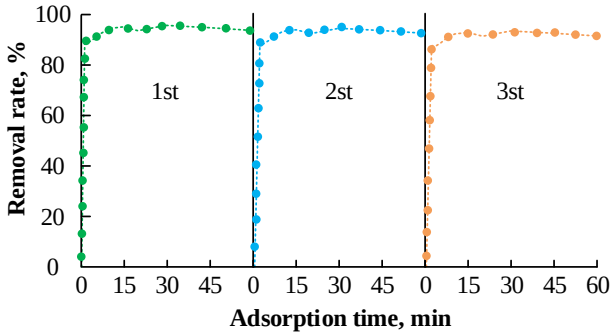

Fig. 13. Experimental results of recyclability of modified nZVI nanomaterials

From Fig. 13, it can be seen that the maximum removal rate of modified nZVI nanomaterials on hexavalent chromium is 96.97 % when used for the first time. After 2 and 3 cycles of use, the maximum removal rates of modified nZVI nanomaterials were 95.23 % and 94.73 %, respectively. It can be seen that after 3 cycles of use, the removal rate of improved nZVI nanomaterials on hexavalent chromium is relatively high, indicating that the material still has high adsorption performance and can be reused multiple times.

The influence of different anions and cations on the adsorption performance of modified nZVI is shown in Fig. 14. In Fig. 14, the concentrations of Ca^{2+}, Mg^{2+}, and Cl^- are all 25 mmol/L, and the concentrations of Mn^{2+}, NO_3^-, and HCO_3^- are 0.5 mmol/L, 2.5 mmol/L, and 5 mmol/L, respectively. From Fig. 14, it can be seen that the removal rate of modified nZVI on hexavalent chromium under Cl^- anion is closer to that before the addition of anions and cations, and the maximum removal rate at this time is 96.53 %, while the removal rate of modified nZVI on hexavalent chromium under Mg^{2+} cation is the lowest. This indicates that different ions have different effects on the adsorption performance of modified nZVI, and cations Ca^{2+}, Mg^{2+} and Mn^{2+} have adverse effects, while anions have little effect on the removal of hexavalent chromium Cr (VI) by modified nZVI.

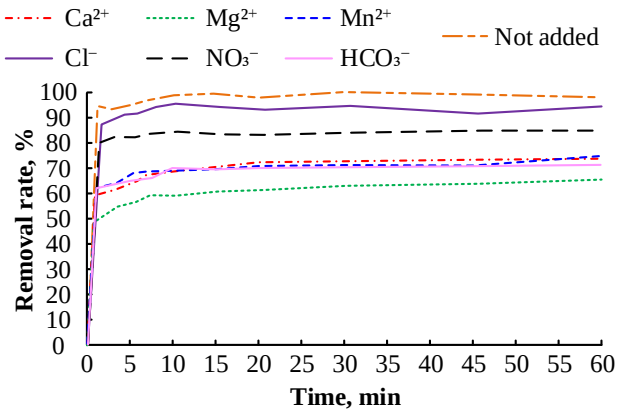

Fig. 14. The influence of different anions and cations on the adsorption performance of modified nZVI

To analyze the effectiveness of modified nZVI nanomaterials in actual wastewater treatment, simulations were conducted on the actual water composition, and the simulation results are shown in Fig. 15.

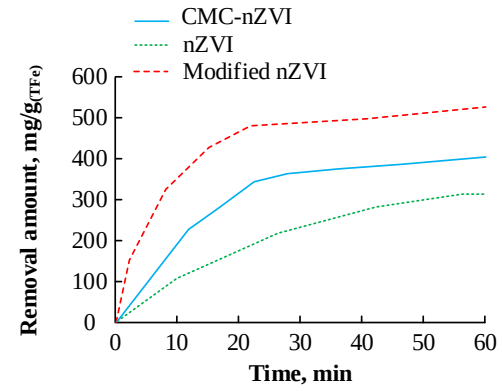

a

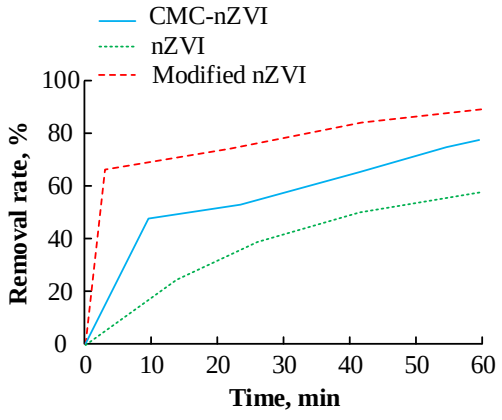

b

Fig. 15. Removal performance of modified nZVI nanomaterials on Cr(VI) in simulated wastewater: a – variation in Cr(VI) removal over time; b – variation in Cr(VI) removal rate over time

From Fig. 15 a, it can be seen that with the increase of time, the removal of Cr(VI) in simulated groundwater by modified nZVI nanomaterials increases synchronously, and the rate of increase gradually slows down. The maximum removal amount of Cr(VI) by modified nZVI nanomaterials is 537.31 mg/g$_{(TFe)}$, which is significantly higher than that of nZVI materials and CMC nZVI materials. According to Fig. 15 b, as time increases, the removal rate of Cr(VI) in simulated groundwater by modified nZVI nanomaterials also increases synchronously, and its corresponding maximum removal rate is 90.25 %. In summary, modified nZVI nanomaterials can also effectively remove Cr(VI) in actual wastewater.

3. DISCUSSION

In order to address heavy metal contamination in groundwater, nZVI material was used, with sulfurization technology and CMC incorporated for modification. This study achieved effective removal of heavy metals from groundwater by modifying nZVI materials, aligning with the findings of scholars such as PlesslK [19], who highlighted the effectiveness of nZVI materials in eliminating heavy metal pollution in groundwater. The results indicated that the modified nZVI nanomaterials achieved an optimal removal rate of hexavalent chromium (96.97 %), and after 3 cycles of reuse, it maintained a removal rate of 94.73 %. Liu et al. reported that CMC-nZVI achieved a U(VI) removal rate of 400 mg/g at pH 3.0 [20]. This study also demonstrates that CMC modification enhances the performance of nZVI materials, which supports the findings of Liu et al.

By comparing the research results of this study with those of other researchers, it is evident that there are both consistencies and differences. The consistency lies in the use of nZVI material, which was modified through CMC. The difference is in the unique combination of sulfurization technology and CMC in this study, which improved the removal efficiency of nZVI for hexavalent chromium. Keochanh found that the removal rates of arsenic using sulfurized nZVI and CMC-nZVI were 41.0 % and 11.0 %, respectively, both lower than the 45.5 % removal rate for bare nZVI [21]. This suggests that the same modification method may not be universally applicable for removing other pollutants.

The findings of this study underscore the effectiveness of modified nZVI nanomaterials in the removal of hexavalent chromium, which can further contribute to advancing scientific knowledge regarding the broader performance of nZVI in removing various pollutants. This, in turn, may facilitate the development of more targeted strategies and promote the application of nZVI materials in complex environmental systems.

4. CONCLUSIONS

Following material characterization, stability testing, analysis of influencing factors, reaction kinetics analysis, regeneration studies, and simulation experiments, several key observations were made. The modified nZVI nanomaterials prepared via the surface corrosion method exhibited a sheet-like shell structure. These modified materials demonstrated more uniform and enhanced properties, achieving a hexavalent chromium removal rate of 96.97 %, indicating superior performance.

FTIR analysis revealed that the fusion of modified nZVI nanomaterials occurs primarily on the surface layer. In

stability testing, the maximum transmittance of suspensions of nZVI, sulfurized nZVI, CMC-nZVI, and modified nZVI nanomaterials were 71.57 %, 59.92 %, 6.89 %, and 2.54 %, respectively. This indicates that sulfurization helps alleviate particle aggregation and settling.

In the analysis of influencing factors, under various sulfurizing agent/iron molar ratios, the removal rate of hexavalent chromium was higher for the modified nZVI nanomaterials compared to sulfurized nZVI, highlighting the improved performance due to CMC modification. The maximum removal rates of the modified nZVI material at temperatures of 0 °C, 18 °C, 25 °C, and 36 °C were 84.58 %, 84.59 %, 96.97 %, and 86.42 %, respectively. At a dosage of 52 mg/L, the minimum hexavalent chromium concentration achieved was 0.01 mg/L, with a removal rate of 96.77 % within 10 minutes of reaction.

The reaction kinetics analysis indicated equilibrium adsorption capacities of 3.570×10^2, 3.570×10^2, 3.923×10^2, and 3.695×10^2 at 0 °C, 18 °C, 25 °C, and 36°C, respectively. In the regeneration study, after 2 and 3 cycles of use, the maximum removal rates of the modified nZVI nanomaterials were 95.23 % and 94.73 %, respectively, suggesting high adsorption performance and the potential for repeated use. In the simulation experiment, the modified nZVI nanomaterials achieved a maximum Cr(VI) removal of 537.31 mg/g (TFe) and a maximum removal rate of 90.25 % in actual wastewater.

In conclusion, the designed modified nZVI nanomaterials demonstrate excellent performance and can effectively remove Cr(VI) from groundwater. However, the research has some limitations, particularly in the context of composite pollution. Groundwater often contains heavy metal pollutants in various forms simultaneously, a factor not fully addressed in this study. Future research could explore removal technologies under conditions of composite pollution and investigate interactions between different pollutants.

Acknowledgments

At the end of this research, I would like to express my heartfelt gratitude to all my friends. Your encouragement will be the driving force for me to continue moving forward. In the future, we will continue to work hard and strive to do better in our future work.

REFERENCES

1. **Liu, S., Wang, Y., Zhang, R., Guo, G., Zhang, K., Fan, Y., Feng, C., Li, H.** Water Quality Criteria for Lanthanum for Freshwater Aquatic Organisms Derived via Species Sensitivity Distributions and Interspecies Correlation Estimation Models *Ecotoxicology* 31 (6) 2022: pp. 897 – 908. https://doi.org/10.1007/s10646-022-02557-z
2. **McEachran, A.R., Dickey, L.C., Rehmann, C.R., Isenhart, T.M., Groh, T.A., Perez, M.A., Rutherford, C.J.** Groundwater Flow in Saturated Riparian Buffers and Implications for Nitrate Removal *Journal of Environmental Quality* 52 (1) 2023: pp. 64 – 73. https://doi.org/10.1002/jeq2.20428
3. **Qi, S., Liu, W., Shu, H., Liu, F., Ma, J.** Soil NO_3^- Storage from Oasis Development in Deserts: Implications for the Prevention and Control of Groundwater Pollution *Hydrological Processes* 34 (20) 2020: pp. 3941 – 3954. https://doi.org/10.1002/hyp.13855
4. **Raja, V., Neelakantan, M.A.** Pollution and Noncarcinogenic Health Risk Levels of Nitrate and Fluoride in Groundwater of Ramanathapuram District, Tamil Nadu, India *International Journal of Environmental Analytical Chemistry* 103 (10) 2023: pp. 2254 – 2269. https://doi.org/10.1080/03067319.2021.1890063
5. **Oehler, T., Ramasamy, M., George, M.E., Babu, S.D.S., Dähnke, K., Ankele, M., Böttcher, M.E., Santos, I.R., Moosdorf, N.** Tropical Beaches Attenuate Groundwater Nitrogen Pollution Flowing to the Ocean *Environmental Science & Technology* 55 (12) 2021: pp. 8432 – 8438. https://doi.org/10.1021/acs.est.1c00759
6. **Naik, M.R., Barik, M., Prasad, K.V., Kumar, A., Verma, A.K., Sahoo, S.K., Jha, V., Sahoo, N.K.** Hydro-geochemical Analysis Based on Entropy and Geostatistics Model for Delineation of Anthropogenic Ground Water Pollution for Health Risks Assessment of Dhenkanal District, India *Ecotoxicology* 31 (4) 2022: pp. 549 – 564. https://doi.org/10.1007/s10646-021-02442-1
7. **Yang, X., Cai, J., Wang, X., Li, Y., Wu, Z., Wu, W.D., Chen, X.D., Sun, J., Sun, S.P., Wang, Z.** A Bimetallic Fe-Mn Oxide-Activated Oxone for In Situ Chemical Oxidation (ISCO) of Trichloroethylene in Groundwater: Efficiency, Sustained Activity, and Mechanism Investigation *Environmental Science & Technology* 54 (6) 2020: pp. 3714 – 3724. https://doi.org/10.1021/acs.est.0c00151
8. **Brumovský, M., Filip, J., Malina, O., Oborná, J., Sracek, O., Reichenauer, T.G., Andrýsková, P., Zbořil, R.** Core-Shell Fe/FeS Nanoparticles with Controlled Shell Thickness for Enhanced Trichloroethylene Removal *ACS Applied Materials & Interfaces* 12 (31) 2020: pp. 35424 – 35434. https://doi.org/10.1021/acsami.0c08626
9. **Huang, S., Yin, Y., Sun, R., Tan, X.** In Situ Anaerobic Bioremediation of Petroleum Hydrocarbons in Groundwater of Typical Contaminated Site in Shanghai, China: A Pilot Study *Environmental Engineering Science* 38 (11) 2021: pp. 1052 – 1064. https://doi.org/10.1089/ees.2020.0534
10. **Ishag, A., Yue, Y., Zhu, W., Li, C., Zhang, B., Huang, X., Sun, Y.** The Removal Mechanism of U(VI) on nZVI/MoS_2 Composites Investigated by Batch, Spectroscopic, and Modeling Techniques *The Journal of Physical Chemistry C* 127 (32) 2023: pp. 15962 – 15968. https://doi.org/10.1021/acs.jpcc.3c04686.s001
11. **Guha, T., Mukherjee, A., Kundu, R.** Nano-Scale Zero Valent Iron (nZVI) Priming Enhances Yield, Alters Mineral Distribution and Grain Nutrient Content of Oryza sativa L. cv. Gobindobhog: A Field Study *Journal of Plant Growth Regulation* 41 (2) 2022: pp. 710 – 733. https://doi.org/10.1007/s00344-021-10335-0
12. **Samarghandi, M.R., Dargahi, A., Zolghadr Nasab, H., Ghahramani, E., Salehi, S.** Degradation of Azo Dye Acid Red 14 (AR14) from Aqueous Solution Using H_2O_2/nZVI and $S_2O_8^{2-}$/nZVI Processes in the Presence of UV Irradiation *Water Environment Research: A Research Publication of the Water Environment Federation* 92 (8) 2020: pp. 1173 – 1183. https://doi.org/10.1002/wer.1312
13. **Ng, W.M., Chong, W.H., Abdullah, A.Z., Lim, J.** Exploring the Impact of Surface Functionalization on the

Reaction, Magnetophoretic, and Collective Transport Behavior of Nanoscale Zerovalent Iron *Langmuir: The ACS Journal of Surfaces and Colloids* 39 (48) 2023: pp. 17270 – 17285. https://doi.org/10.1021/acs.langmuir.3c02358

14. **Li, X., Hao, R., Guo, J., Wang, Y., Gu, K., Fang, S., Liu, H., Sun, S., Wei, G., Ma, X.** Preparation of a Large-Grained Cu_2ZnSnS_4 Thin-Film Absorbent Layer by Two-Cycle Deposition Sulfurization *Journal of Electronic Materials* 50 (10) 2021: pp. 5590 – 5598. https://doi.org/10.1007/s11664-021-09135-9
15. **Hong, J.E., Jung, Y., Min, D., Jang, M., Kim, S., Park, J., Park, Y.** Visible-Light-Induced Organophotocatalytic Difunctionallization: Open-Air Hydroxysulfurization of Aryl Alkenes with Aryl Thiols *The Journal of Organic Chemistry* 87 (11) 2022: pp. 7378 – 7391. https://doi.org/10.1021/acs.joc.2c00595
16. **Ma, J., Jia, N., Jin, H., Yao, S., Zhang, K., Kai, Y., Wu, W., Wen, Y.** Chitosan Induced Synthesis of Few-layer MoS_2/Fe-doped Biochar and Its Dual Applications in Cr(VI) Removal *Separation and Purification Technology* 317 2023: pp. 123880. https://doi.org/10.1016/j.seppur.2023.123880
17. **Bashiri, H., Javanmardi, A.H.** Investigation of Fractal-like Characteristics According to New Kinetic Equation of Desorption *Langmuir: The ACS Journal of Surfaces and Colloids* 37 (6) 2021: pp. 2123 – 2128. https://doi.org/10.1021/acs.langmuir.0c03240
18. **Pang, J., Wang, Z., Zhang, J., Zhang, S., Hu, P., Rao, J.** Behavior and Kinetic Mechanism Analysis of Dissolution of Iron Ore Particles in HIsmelt Process Based on High-temperature Confocal Microscopy *ISIJ International* 63 (3) 2023: pp. 448 – 454. https://doi.org/10.2355/isijinternational.ISIJINT-2022-261
19. **Plessl, K., Russ, A., Vollprecht, D.** Application and Development of Zero-valent Iron (ZVI) for Groundwater and Wastewater Treatment *International Journal of Environmental Science and Technology* 20 (6) 2023: pp. 6913 – 6928. https://doi.org/10.1007/s13762-022-04536-7
20. **Liu, Y., Zhang, H., Ding, Y., Hu, N., Ding, D.** Preparation of Carboxy Methyl Cellulose Stabilized Nano-Sized Zero-Valent Iron and its Properties for in Situ Remediation of Groundwater in Areas After Acid in Situ Leach Uranium Mining *Environmental Science: Water Research & Technology* 9 (5) 2023: pp. 1480 – 1490. https://doi.org/10.1039/D2EW00977C
21. **Keochanh, D., Tongkamnoi, S., Phenrat, T.** Can Polymeric Surface Modification and Sulfidation of Nanoscale Zerovalent Iron (NZVI) Improve Arsenic-contaminated Agricultural Soil Restoration Via Ex Situ Magnet-assisted Soil Washing? *Environmental Chemistry* 20 (7) 2024: pp. 302 – 318. https://doi.org/10.1071/EN23078